Interdomain Interactions Modulate the Active Site Dynamics of Human Inducible Nitric Oxide Synthase

Journal:	*The Journal of Physical Chemistry*
Manuscript ID	jp-2022-04091p.R1
Manuscript Type:	Special Issue Article
Date Submitted by the Author:	16-Aug-2022
Complete List of Authors:	Tumbic, Goran; Indiana University Bloomington Li, Jinghui; Yantai Institute of Coastal Zone Research (YIC), Chinese Academy of Sciences (CAS) Jiang, Ting ; University of New Mexico College of Arts and Sciences Hossan, Md Yeathad ; Indiana University Bloomington Feng, Changjian; University of New Mexico, College of Pharmacy Thielges, Megan; Indiana University Bloomington, Department of Chemistry

Interdomain Interactions Modulate the Active Site Dynamics of Human Inducible Nitric Oxide Synthase

Goran W. Tumbic,[a] Jinghui Li,[b] Ting Jiang,[b] Md Yeathad Hossan,[a] Changjian Feng,[b] Megan C. Thielges*[a]*

[a] Indiana University, Department of Chemistry, Bloomington, IN 47405, United States

[b] University of New Mexico, Department of Pharmaceutical Sciences, Albuquerque, NM 87131, United States

KEYWORDS infrared spectroscopy, 2D IR spectroscopy, interdomain electron transfer, protein dynamics, nitric oxide synthase

ABSTRACT

Nitric oxide synthase (NOS) is a homodimeric flavohemoprotein responsible for catalyzing the oxidation of L-arginine (L-Arg) to citrulline and nitric oxide. Electrons are supplied for the reaction via interdomain electron transfer between an N-terminal heme-containing oxygenase domain and a FMN-containing (sub)domain of a C-terminal reductase domain. Extensive attention has focused on elucidating how conformational dynamics regulate electron transfer between the domains. Here we investigate the impact of interdomain FMN-heme interaction on the heme active site dynamics of human inducible NOS (iNOS). Steady state linear and time-resolved two-dimensional infrared (2D IR) spectroscopy was applied to a CO ligand at the heme within the oxygenase domain for full length and truncated or mutated constructs of iNOS. Whereas the linear spectra of the CO ligand were identical among the constructs, 2D IR spectroscopy revealed variation in the frequency dynamics. The constructs that can form the docked state due to the presence of both the FMN and oxygenase domains showed slower dynamics than the oxygenase domain alone. Introduction of the mutation (E546N) predicted to perturb electrostatic interactions between the domains resulted in measured dynamics intermediate between those for the full length and individual oxygenase domain, consistent with perturbation to the docked/undocked equilibrium. These results indicate that docking of the FMN to the oxygenase domains not only brings the FMN cofactor within electron transfer distance of the heme domain, it also modulates the dynamics sensed by the heme ligand within the active site in a way expected to promote efficient electron and proton transfer.

Introduction

Production of the ubiquitous signaling molecule nitric oxide (NO) by NO synthase (NOS) underlies diverse physiological responses such as vasodilation and neurotransmission.[1, 2] Extensive attention has been directed toward elucidating the mechanism of NOS catalysis and regulation.[3-5] Conformational changes control NOS turnover by bringing together distinct domains of the enzyme and enabling electrons to shuttle successively between them.[6-8] Here we report evidence that docking of domains not only brings cofactors within sufficient proximity for electron transfer (ET) but also alters the dynamics within the catalytic heme domain in a way that would promote inter-domain electron transfer (IET).

NOS generates NO through oxidation of the guanidyl side chain of L-arginine (L-Arg) with uptake of molecular oxygen, consumption of NADPH, and release of citrulline. Each subunit of the homodimeric enzyme has two domains (Figure 1a).[3] An N-terminal oxygenase domain (NOS_{oxy}), the site of L-Arg oxidation, contains a heme prosthetic group and a 6R-5,6,7,8-tetrahydrobiopterin (H_4B) cofactor. A C-terminal reductase domain is composed of FMN and FAD/NADPH binding subdomains. The oxygenase and reductase domains are connected by a linker that binds calmodulin (CaM). This overall architecture is shared by the three mammalian NOS isoforms: endothelial NOS (eNOS), neuronal NOS (nNOS), and inducible NOS (iNOS). The linker of iNOS, however, tightly binds CaM at a basal level of Ca^{2+}, while binding of CaM to the linker of nNOS and eNOS occurs upon increase in intracellular [Ca^{2+}].

The complex series of steps underlying NO production within the oxygenase domain requires uptake of three electrons. The electrons enter the reaction from NADPH by reduction of the FAD subdomain. The electrons are then transported from FAD to FMN cofactors between subdomains within the reductase domain. The next step, the transfer of electrons from the

reductase domain to the oxygenase domain, governs overall production of NO.[7] A conformational change of the enzyme dissociates the FMN subdomain from the FAD domain and docks it with the oxygenase domain of the other NOS monomer.[8, 9] Upon association of the domains, the FMN subdomain supplies electrons for NO production within the oxygenase domain. The conformational change involves large rearrangement in the molecular architecture of the enzyme. An extended "input" state, intermediate states, and a compact "output" state in which the FMN domain is in contact with the oxygenase domain have been observed for full-length NOS proteins by cryo-electron microscopy (cryo-EM).[10] Binding of CaM to the linker region of NOS induces the conformational change from the input state to the output state, so it acts as a "molecular switch" that enables electron flow from NADPH, through the FAD and FMN cofactors, to the heme within the oxygenase domain.[11, 12] In the presence of CaM, off-pathway electron transfer is minimized; activation of NOS by CaM binding can rapidly trigger NO production.

Upon association of the FMN and oxygenase domains, a path for efficient electron transfer from the FMN cofactor to the heme center is presumably established. While the crystal structures of only the individual oxygenase and reductase domains have been solved, the docking interface between the FMN and heme domains within the NOS output state has been mapped by hydrogen deuterium exchange mass spectrometry to the surface area surrounding the FMN cofactor.[13] The interface is maintained primarily by electrostatic interactions between the negatively charged surface of the FMN domain and a positively charged patch on the oxygenase domain. Charge neutralization and reversal mutations along the FMN subdomain of the reductase domain or the heme domain for nNOS significantly slow heme reduction.[14-18] One of the involved residues is a conserved glutamic acid (E762 in rat nNOS, E546 in human iNOS) located near the FMN cofactor in the FMN subdomain. When the residue is mutated in iNOS (E546N), the FMN-heme IET is

noticeably diminished due to a larger entropic activation barrier compared to the wild type.[19] Pulsed EPR data indicate that the charge neutralization mutation decreases the frequency of contact between the FMN and heme domains.[19, 20] In agreement, a charge reversal mutation at another surface residue in murine iNOS (E546R) leads to perturbation of the interaction between the FMN and heme domains.[13]

While evidence increasingly supports that association of the FMN and heme domains is required for establishing a productive pathway for the FMN-heme IET, little is known about whether and how the complexation otherwise impacts the oxygenase domain and its functionality for subsequent chemistry at the heme center. Toward investigating this question, herein we have employed CO ligated to the ferrous heme as a probe of the active site of the oxygenase domain. CO-ligated NOS acts as a stable mimic of the dioxygen (O_2) bound heme intermediate.[21] Heme-ligated CO is well developed as a probe of hemoprotein active sites via linear and two-dimensional infrared (IR) spectroscopy.[22-24] The vibrational frequency of CO is sensitive to hydrogen bonding and the local electric field, providing a reporter of the interactions felt within an enzyme active site. When ligated to the heme center of NOS, in the presence of the L-Arg substrate, the CO participates in H-bonding with the L-Arg side chain and an active site water molecule (Figure 1b).[21, 25] We thus anticipate the CO vibrational frequency to be highly sensitive to any changes in these specific H-bonding interactions.

To some extent, interaction with the polarization field from all parts of the protein and solvent affects the CO vibration. Furthermore, an enzyme active site exists as an ensemble of conformational states, among which the CO ligand experiences a distribution of environments. The heterogeneity of the interactions of the CO can be captured by FT IR spectroscopy through inhomogeneous line-broadening of the vibrational absorbance. 2D IR spectroscopy enables more

rigorous measure of the frequency inhomogeneity and, moreover, the underlying dynamics. Knowing the dynamics among the states that underlie the inhomogeneity provides insight into the molecular origins of the heterogeneity.

To assess the impact of docking the FMN domain on the active site of the oxygenase domain, we compared full-length human iNOS ($iNOS_{FL}$) to a truncated construct consisting of only the oxygenase domain ($iNOS_{oxy}$), which lacks the FMN domain and thereby cannot form the output state. We also characterized a bi-domain oxygenase/FMN construct (oxyFMN) containing only the FMN subdomain (i.e., the FAD/NADPH subdomain is absent), along with the CaM-binding linker and the oxygenase domain. This construct removes possible interaction between the FAD and FMN domains to promote association of the FMN and heme domains. The oxyFMN construct is an established model of the output state of NOS. The cryo-EM density of this construct can be fitted without any alteration of the cryo-EM density of the holoprotein, showing that the structure of the docked complex is similar for the oxyFMN and full-length NOS proteins.[10] Finally, to assess the consequences of a properly aligned FMN domain with the oxygenase domain in the wild type (wt) proteins, we characterized E546N oxyFMN ($iNOS_{E546N}$), which perturbs FMN to oxygenase domain docking.[19, 26] CaM exists in the purified oxyFMN and full-length iNOS proteins.

We have found that, although the vibration of CO ligands to heme proteins are in general exquisitely sensitive to interaction with their environment, the FT IR absorption spectra of the CO ligand of the iNOS constructs are nearly identical. Despite this observation, 2D IR spectroscopy of the CO ligand surprisingly reveals that docking of the FMN domain alters the dynamics sensed within the oxygenase domain. The inhomogeneous distribution of vibrational frequencies of the CO ligand arises from states that interconvert more slowly in the constructs in which association

of the FMN and heme domains is possible. These results argue docking of the FMN domain not only brings the FMN cofactor within ET distance of the heme domain, it also modulates the dynamics sensed by the heme ligand within the active site. To our knowledge, this is the first detailed spectroscopic investigation of the modulation of NOS protein active site local dynamics by interdomain interactions.

Materials and Methods

Expression and purification of the human iNOS proteins were performed as described.[19, 26] Each protein sample was loaded between two CaF_2 windows separated by a 76 μm spacer. Visible spectra (Agilent Cary 300 Spectrometer) and FT IR spectra (Agilent Cary 670 FT-IR spectrometer) of all samples were recorded to ensure binding of CO. Details regarding procedure of protein identification by mass spectrometry, Fe(II)–CO sample preparation, FT-IR spectral acquisition, and subsequent processing are provided in the Supporting Information. 2D IR spectroscopy was conducted in the traditional BOXCARS geometry as previously described; see Supporting Information for a complete description.[27-29] The center line slope (CLS) analysis of the T_w-dependent 2D IR spectra along with fitting to the linear spectra was used to determine FFCFs parameters.[30, 31] Experiments were performed in triplicate with independently prepared samples, except for the full length protein, for which we were only able to obtain duplicate data.

Results

The FT IR spectra of the CO-ligated iNOS constructs are nearly indistinguishable (Figure 2). Both the center frequencies and linewidths vary only slightly (~0.1 cm^{-1}); see Table 1. All spectra show a Gaussian band corresponding to the CO stretching mode at 1904 cm^{-1} with a full-

width-at-half maximum of ~8.4 cm^{-1}, which is in good agreement with prior FT IR spectroscopy of full length iNOS.[21] Thus, the FT IR spectra do not distinguish any differences in the environment of the CO ligand among the constructs. These results suggest that the H-bonding interactions between the ligated CO and L-Arg substrate are not strongly affected by docking of the reductase domain.

To gain deeper insight into the ensembles, we applied 2D IR spectroscopy to the CO-ligated constructs (Figure 3). The 2D IR spectra correlate vibrational frequencies excited before (horizontal axis) and detected after (vertical axis) a waiting time (T_w).[32] When 2D spectra are acquired with very short T_w, before the protein has time to move, the frequencies of the CO within the ensemble initially excited and later detected are the same, leading to 2D absorbance peaked along the diagonal and a diagonally elongated line-shape. The diagonal elongation provides a measure of the inhomogeneous broadening of the band arising from heterogeneity among the ensemble distribution. As T_w is increased, the dynamics among the inhomogeneous distribution result in evolution of the 2D IR spectral line-shape. After the CO ligand samples available states, the final frequencies become different from the initial frequencies, leading to growth of off-diagonal 2D amplitude and less elongated 2D lineshape. Thus, the lineshape evolution directly follows the frequency dynamics and, accordingly, the dynamics among the underlying states.

The T_w-dependent changes in the 2D IR spectral lineshapes for the CO-ligated iNOS constructs were analyzed via a standard metric for band elongation, the CLS.[30, 31] The CLS for 2D spectra taken with a T_w of zero can vary from 1 to 0, reflecting the extent of inhomogeneous broadening. The T_w-dependent CLS decays (Figure 4a) are used in combination with fitting to the linear spectra to obtain frequency-frequency correlation functions (FFCFs) that describe the CO lineshape broadening and frequency dynamics (Table 1). Briefly, the CLS decay is assumed to

reflect the normalized inhomogeneous contribution to the FFCF. The initial value of the CLS decay provides the relative contributions of homogeneous and inhomogeneous broadening. Line-broadening due to homogeneous dynamics that are fast on the IR timescale (i.e., $\Delta\tau << 1$) are described by a homogeneous linewidth (Γ). The time dependence of the CLS delay reveals the dynamics among the inhomogeneous distribution. The inhomogeneous dynamics for the CO ligand of the iNOS constructs were modeled by two timescales: frequency deviation (Δ_f) due to states sampled on a fast (4-10 ps) timescale, τ, and frequency deviation (Δ_s) from states sampled on timescales longer than the experimental window (~20 ps), which manifest as an offset.

First consider the 2D IR data for $iNOS_{oxy}$, the construct consisting of only the oxygenase domain. The 2D IR spectrum at T_w of 0.25 ps is highly elongated along the diagonal; at T_w of 10 ps the 2D lineshape becomes less diagonally elongated due to growth in off-diagonal amplitude from exchange between the underlying states. The CLS decay that follows the lineshape evolution is shown in Figure 4a. The FFCF derived from the data indicates about equal inhomogeneous frequency deviation is sampled on the rapid (Δ_f =2.1 cm^{-1}) and slower (Δ_s=2.2 cm^{-1}) timescales (Table 1). Thus, the heterogeneity of environments of the CO ligand in the individual oxygenase domain arises from about equal contributions of rapidly and slowly interconverting states.

Despite similar linear FT IR spectra of the CO ligand among the constructs (Figure 2), 2D IR spectroscopy reveals distinct dynamics (Figure 3). In comparison to the 2D IR data for $iNOS_{oxy}$, the evolution of the 2D line shape is slower for full-length $iNOS_{FL}$ in which the oxygenase domain can dock with the FMN domain. Although the initial elongation of the 2D lineshapes for the constructs is about the same, the CLS decay for $iNOS_{FL}$ shows an initial decay over a ~3 ps timescale, then remains constant at a relatively large offset. The difference in the extent of spectral evolution between the constructs can be seen clearly by comparison of the 2D band shapes and

CLS for T_w of 10 ps (Figure 3). At this T_w, the CLS reflecting the extent of diagonal elongation for $iNOS_{FL}$ is noticeably lower than $iNOS_{oxy}$. Corresponding with the slower CLS decay, the FFCF for $iNOS_{FL}$ indicates that the inhomogeneous dynamics overall are slower (Table 1). Whereas for $iNOS_{oxy}$ the inhomogeneous frequency deviation is equally sampled on rapid and slow timescales, for $iNOS_{FL}$ nearly twice as much is sampled on the slower (Δ_s=2.8 cm^{-1}) than rapid (Δ_f =1.4 cm^{-1}) timescale (Table 1). Thus, in comparison to the individual oxygenase domain, the heterogeneity of states reported by the CO ligand in the full-length enzyme interconvert more slowly.

2D IR spectroscopy of iNOS oxyFNM, the construct containing only the FMN and heme domains, shows identical results as $iNOS_{FL}$. The CLS decays overlay within error (Figure 4a). As for $iNOS_{FL}$, the FFCF for iNOS oxyFMN indicates about twice as much inhomogeneous frequency deviation sampled on the slower (Δ_s=2.8 cm^{-1}) than the rapid (Δ_f =1.4 cm^{-1}) timescale (Table 1).

Introduction of the E546N mutation perturbs the dynamics of iNOS. The 2D lineshape for $iNOS_{E546N}$ at the shortest T_w is more elongated than the other constructs. This results in the larger initial value of the CLS decay. The FFCF indicates that the contribution from homogeneous broadening, which results from very fast (i.e., $\Delta\tau << 1$) fluctuations, is lower for the mutant than the other wt constructs. A second significant effect of the mutation is the change in the CLS decay, reflecting impact to the inhomogeneous dynamics. In comparison to wt oxyFMN, the CLS for the E546N mutant decays much more rapidly. The FFCF parameters for $iNOS_{E546N}$, including frequency deviation amplitudes and timescale, are intermediate between those for $iNOS_{FL}$ and $iNOS_{oxy}$ (Table 1). Of note is that the LC-MS/MS data (Figures S1-S2) have confirmed that intactness of the wild type and E546N mutant iNOS oxyFMN proteins and the E→N mutation, showing that the observed difference in 2D IR is not due to protein truncation.

Given the intermediate FFCF parameters obtained for $iNOS_{E546N}$, we considered whether the 2D data could be modeled assuming a superposition of states reflective of the $iNOS_{oxy}$ and $iNOS_{FL}$/iNOS oxyFMN constructs. To model the two components, 2D IR data can be fit to the weighted sum of the FFCFs for the components.[33] To account for the higher initial CLS observed for $iNOS_{E546N}$ (Figure 4a), indicative of less homogeneous broadening, we subtracted the difference in the initial CLS value from $iNOS_{FL}$ and $iNOS_{oxy}$. The inhomogeneous dynamics reflected by the shifted CLS decay for $iNOS_{E546N}$ was then fit to a superposition of contributions from the FFCF for the $iNOS_{FL}$ and $iNOS_{oxy}$ states (Figure 4b). This analysis yields that $iNOS_{E546N}$ populates 10-20% of the wt $iNOS_{FL}$/iNOS oxyFMN and 80-90% of the $iNOS_{oxy}$ states.

Discussion

We analyzed how the docking of the FMN domain impacts the active site within the oxygenase domain. CO ligated to the heme within the oxygenase domain of iNOS, a stable model for the physiological O_2 complex, served as a vibrational probe of the active site. To characterize iNOS in the conformational states adopted during enzymatic turnover, analysis was directed at full length, truncated, and the E546N mutant of iNOS. FT IR spectra of the CO ligand in these constructs are nearly identical, showing a single Gaussian absorbance at 1904 cm^{-1} with a full-width-at-half-maximum of 8.4 ± 0.1 cm^{-1}. The observation of a narrow band at this frequency in the L-Arg bound state of both full length and the truncated iNOS is in agreement with prior FT IR and resonance Raman (rR) spectroscopy.[21, 34, 35] The consistent center frequency and line width across iNOS constructs indicates that formation of the output state does not substantially perturb the average or heterogeneity of interactions of the CO with environment of the oxygenase active site.

Vibrational spectroscopy of CO ligands is a well-established approach to characterize the hemeprotein environments.[23, 24, 36] Hydrogen bonding or electrostatic interactions of the ligand with the protein environment modulate back-bonding from the π^* orbital of CO to the heme Fe *d* orbitals, altering the vibrational frequency.[22, 23] For example, the frequency of CO ligated in myoglobin depends on hydrogen bonding to a histidine residue (H64). The frequency downshifts by 8 cm^{-1} for a homolog with a stronger glutamine donor, whereas the frequency upshifts when a hydrophobic residue replaces H64.[22] When CO is ligated to iNOS, the vibrational frequency of 1904 cm^{-1} is notably very low in comparison to the frequencies observed in the absence of the L-Arg substrate (~1930 and 1950 cm^{-1}),[21] as well as among hemeproteins in general (~1900-1980 cm^{-1}).[23, 37] The low frequency of 1904 cm^{-1} is attributed to H-bonding interactions with both the L-Arg substrate and an active site water molecule. A similarly low frequency of 1908 cm^{-1} is found for the CO ligated to nematode hemoglobin, where two hydrogen bond donors, a distal Gln and Tyr residue, are directed at the CO ligand.[38] The hydrogen bonding interactions among CO, L-Arg, and an active site water are observed in the crystal structures of the nNOS isoform (Figure 1b) and also supported by temperature-dependent shift in the vibrational frequency of ligated CO in iNOS.[21] In addition, prior IR spectroscopy indicates that the network of H-bonding among the CO, L-Arg, and water is cooperative.[39] Higher frequencies that indicate weaker hydrogen bonding of the CO ligand are observed when the L-Arg substrate is replaced by analogs with side chains that provide stronger hydrogen bond donors, thus arguing that competing interaction of the analogs with active site water reduces hydrogen bonding to the CO ligand. Despite the delicate hydrogen bonding interactions within the iNOS active site, the CO vibration was insensitive to removal of the FMN domain (Figure 2). The insensitivity suggests that the balance of H-bonding interactions among the CO, L-Arg, and water molecule are not affected by the interdomain FMN-heme

docking. These results, along with the rR data,[19] indicate that the docking of the FMN domain to the heme domain does not notably affect the average electronic and structural properties of the ground state of the heme active center. However, it is possible that docking affects the ensemble but does not generate a net change to the CO frequency distribution to be detectable by the linear IR absorbance. This clearly demonstrates the additional insight provided by 2D IR methods that allow for a more rigorous analysis of the linewidth and frequency dynamics.

While the linear spectroscopic methods are insensitive to interdomain docking, 2D IR spectroscopy does reveal clear changes in the dynamics of the heterogeneity sensed by the CO ligand within the oxygenase domain upon docking of the FMN domain (Figure 4a, Table 1). The total frequency variance (Δ^2) due to inhomogeneous broadening is slightly greater in the constructs ($iNOS_{FL}$ and wt oxyFMN) capable of forming the properly docked FMN/heme state. This observation indicates that the CO ligand experiences greater heterogeneity in the docked state. A more substantial difference among the constructs was found in the frequency dynamics. Specifically, comparison of the FFCFs of $iNOS_{FL}$ and wt oxyFMN to $iNOS_{oxy}$ show a decrease in frequency deviation amplitude associated with states sampled on a few picoseconds and an increase in those sampled on long (> 20 ps) timescales. Thus, docking of the FMN domain increases the population of states with greater energy barriers to interconversion, because either the energy barriers become higher or a subset with greater or lower barriers are favored or disfavored, respectively, in the output state.

The FFCF for $iNOS_{oxy}$ construct reflects the ensemble when all the population adopts the undocked input state. Since none of the constructs adopts exclusively the docked output state, no information is available about the FFCF to rigorously deconvolute the populations of docked and undocked states in the constructs. However, if the assumption is made that the frequency variance

associated with rapid motions (Δ_f) for the $iNOS_{FL}$ and oxyFMN constructs is solely reflective of the undocked state, the population of the docked state is estimated to be 55% (since the variances Δ^2 of inhomogeneous broadening are additive). In the case that the FFCF of the docked state includes rapid inhomogeneous dynamics, the estimate for the docked state would be higher. In comparison, relaxation-induced dipolar modulation enhancement (RIDME) spectroscopy estimates population of 15% for the docked state for the CaM-bound nNOS oxyFMN construct.[40] The discrepancy in the estimates could arise from the differences between the isoforms studied or the redox states of the proteins. In addition, the studies analyzed different aspects of the enzyme structure. The pulsed EPR experiments are sensitive to approach of the heme in the oxygenase domain and spin labels introduced into CaM, while the 2D IR spectroscopy is sensitive to perturbation of the CO ligand within the oxygenase domain.

Truncation of the FAD/NADPH subdomain of the reductase domain results in no change to the dynamics reported by 2D IR spectroscopy of the CO ligand in the oxyFMN construct, compared to the full-length protein (Table 1). This result is rather surprising, as it would indicate that the equilibrium between the input state in which the FMN domain interacts with the FAD/NADPH domain and the free undocked state of the FMN domain may not influence the equilibrium of its docking with the oxygenase domain. On the other hand, comparison of the full length and oxyFMN iNOS proteins by flavin fluorescence lifetime finds only ~2 % docked output state in the full length and a large increase in the population to 25-30% in the oxyFMN.[41] The population of the docked state estimated by fluorescence is particularly much lower. Of note is that the 90 ps component associated with the input state is very close to the lifetime detection limit of the single-photon counting fluorescence lifetime spectrometer, and the estimation of population by fluorescence lifetime should be complemented by other techniques. The fluorescence lifetime

measurements are sensitive to states with close proximity of the FMN cofactor and the heme center, since the signals depend on interaction of the FMN cofactor with the paramagnetic ferric heme center. If the FMN domain contacts the oxygenase domain, but the FMN cofactor does not closely approach the heme center, the population will not be detected as a docked state in the fluorescence lifetime and EPR measurements. However, since the FMN and oxygenase domains are still in contact, the docking effect on 2D IR may still be present. This possibility reduces the expected difference between oxyFMN and full-length proteins in the 2D IR measurements. Alternatively, it is possible that the FFCFs determined by 2D IR are not sufficiently sensitive to detect the small population shift caused by the existence of the FAD/NADPH domain. We also point out the difference in the redox states of the samples in the experiments. Both the fluorescence lifetime and pulsed EPR measurements cited above analyzed as-isolated ferric protein, while the current study examines ferrous protein. Molecular dynamics simulations indicated that the FMN-heme docking is redox state dependent,[42] and it is possible that the different oxidation state of NOS samples affects the conformational equilibrium.

In contrast to removal of the FAD/NADPH domain, mutation of the charged residue E546 leads to substantial perturbation to the dynamics measured by 2D IR spectroscopy. Located at the edge of the FMN domain of human iNOS, E546 is a conserved surface residue that guides the interaction with the oxygenase domain.[17, 18] The CO frequency dynamics for $iNOS_{E546N}$ decay at a rate intermediate between the full-length protein and the individual oxygenase domain. This observation is consistent with the interpretation that the mutation shifts the equilibrium toward the undocked state. Modeling the 2D IR data for $iNOS_{E546N}$ as a superposition of the states of $iNOS_{FL}$ and $iNOS_{oxy}$ estimates that $iNOS_{E546N}$ populates 10-20% full-length and 80-90% NOS_{oxy}-like states, indicating that the mutation shifts the ensemble toward the undocked state (Figure 4b). This

result is anticipated since the E546 residue facilitates the FMN-heme docking by electrostatic interactions. Such putative perturbation by this mutation is based on prior studies by pulsed EPR spectroscopy and the increased entropic barrier to ET based on temperature-dependent kinetics.[19] Our work herein reveals that the mutation also decreases the homogeneous broadening (Table 1), indicating that a rapid fluctuation is suppressed. Since the mutation is on the FMN domain and the CO ligand is in the oxygenase domain, the decreased homogeneous broadening of the CO must arise from perturbation to the docked state. The removal of fluctuations of the charged side chain of E546 itself explains the decreased homogeneous broadening, however another possibility is that rapid fluctuations are suppressed within the oxygenase domain closer to the CO ligand. In either case, the results indicate that perturbation of interactions at the interface of the domains is transmitted to the active site within the oxygenase domain.

The few picoseconds timescale of the suppressed motions in the constructs capable of FMN-oxygenase domain docking implicates rapid fluctuations. To some extent, the CO vibration reflects its interaction with all parts of the proteins and solvent. Considering the sensitivity of the CO frequency to H-bonding, fluctuations in the strong, short-range interactions of the CO and the water and/or L-Arg substrate would substantially influence the CO frequency dynamics. However, the observation that docking does not affect the steady state linear IR spectrum suggests that the hydrogen bonding interactions are not greatly perturbed. An alternate explanation is a change in the water or coupled water dynamics at the protein surface. Theoretical consideration of spectral diffusion by analysis of MD simulations of CO ligated to myoglobin finds that rapid fluctuations of surface water and coupled solvent-protein motion cause rapid fluctuations in the electric field sensed at the CO within the heme pocket.[43, 44] The individual interactions with the CO are weaker, but there are many of them. The observation of slower dynamics in the constructs capable of

forming the output state is consistent with displacement of rapidly fluctuating water solvent at the surface of the oxygenase domain. Perturbation of the mobile water layer by addition of trehalose or fructose similarly leads to slower spectral dynamics for CO ligated by hemoglobin, myoglobin, H64V myoglobin, and M61A cytochrome C552.[44, 45] CO vibrations of metal carbonyl side chain probes similarly report faster spectral dynamics when attached at surface-exposed than buried locations and sensitivity to the addition of viscogens and crowding agents,[46, 47] supporting that rapid water and solvent-coupled vibrations contribute to the spectral dynamics. Irrespective of the molecular origins, our observation that formation of the output state of oxyFMN and iNOS$_{FL}$ proteins results in slower dynamics sensed by the CO ligand indicates that docking of the FMN domain leads to changes transmitted from the surface into the active site of the oxygenase domain. Future analysis of the contributions of fluctuations of the L-Arg, active site water, surface water, and coupled protein motions to the electric field at the CO can better illuminate the molecular origins of the spectral diffusion of the CO ligand of iNOS.

The question arises whether the slower motions of the docked oxygenase domain detected by 2D IR spectroscopy have functional consequences. Docking not only brings redox centers in proximity but can also lead to the release of the solvent and formation of close protein-protein contacts. The desolvation should reduce the number of through space hops by eliminating electron transfer between water molecules and introduce Van der Waals interactions among the cofactors and protein side chains that would promote ET between them.[48-51] Such changes are consistent with the slower dynamics measured for the constructs capable of forming the docked state, and we speculate could promote efficient tunneling pathways. The model of the docked state and prior functional studies for iNOS suggest that ET from the FMN domain to the heme in the oxygenase domain is mediated by a conserved Trp residue (Trp366 in iNOS).[10] The carbonyl backbone of

Trp366 forms a H-bond with the L-Arg substrate, while the aromatic sidechain stacks with the heme group.[25] Stronger Van der Waals interactions from tight packing of Trp366 with the oxygenase heme cofactor, L-Arg substrate, and the FMN domain would enhance coupling through the ET pathway.

Another possible consequence of the slower fluctuations associated with the slower inhomogeneous dynamics measured for the iNOS constructs capable of forming the docked output state is a decrease in the reorganization energy of ET. While 2D IR spectroscopy is not able to capture the timescale of the slow component of the dynamics, if the timescale of motion becomes slower than the ET reaction, the contribution of the motion to reorganization energy would be eliminated.[50, 52-54] Such minimization of reorganization energy through protein-protein interactions provides a possible mechanism to increase specificity in biological ET. Due to the critical function of NOS for production of the signaling molecule NO, the additional control of ET through domain association would serve to optimize signaling fidelity by minimizing undesired side reactions.

Conclusion

In this work, we used CO ligated to the heme center of the oxygenase domain to probe the active site in iNOS constructs with varying ability to form a docked, output state. The ability to form the docked state had no effect on the average electrostatic or hydrogen bonding interactions of the CO, as evident from the identical linear FT IR spectra among the constructs. 2D IR spectroscopy, however, revealed that the fluctuations sensed by the CO ligand are impacted by docking. Slower dynamics associated with greater rigidity in the docked state could facilitate ET pathways or reduce reorganization energy. Significantly, the study reveals how docking

interactions at the oxygenase surface are transmitted to changes in the fluctuations sensed at the active site with potential implications to catalysis.

FIGURES

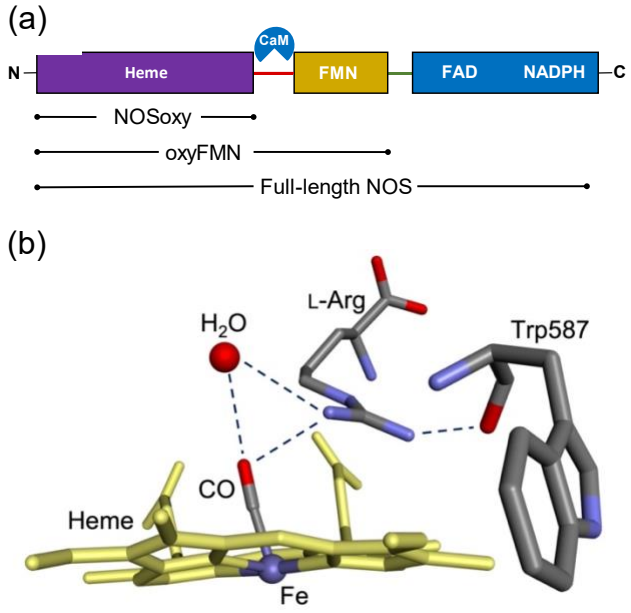

Figure 1. (a) Schematic representation of the full-length NOS protein depicting its oxygenase and reductase domains, and CaM-binding region that connects the two domains. The FMN (yellow) and FAD/NADPH subdomains (blue) in the reductase domain are illustrated. The NOS constructs used in this work are also depicted. (b) The heme active site in the Fe(II)-CO complex of L-Arg bound rat nNOS oxygenase domain (pdb ID 2G6M). The hydrogen bonds around the CO ligand are shown in dashes. Rat nNOS Trp587, the equivalent residue of murine iNOS Trp366, forms a hydrogen bond with the bound L-Arg substrate via its backbone carbonyl oxygen atom. The heme active site structures among the NOS isoforms are highly conserved.

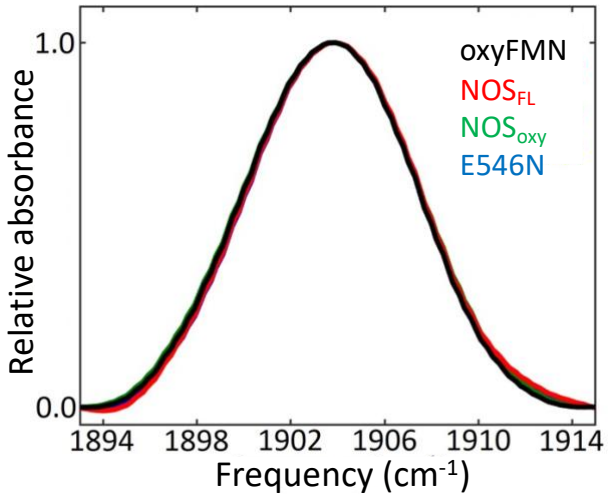

Figure 2. FTIR spectra of the CO ligand of iNOS constructs oxyFMN (black), NOS_{FL} (red), NOS_{oxy} (green), and $iNOS_{E546N}$ (blue).

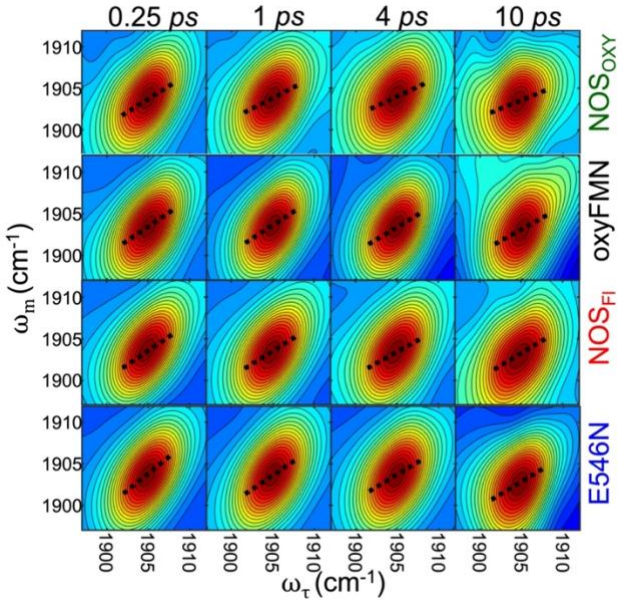

Figure 3. Example T_w-dependent 2D IR spectra of oxyFMN, NOS_{FL}, NOS_{oxy}, and E546N iNOS.

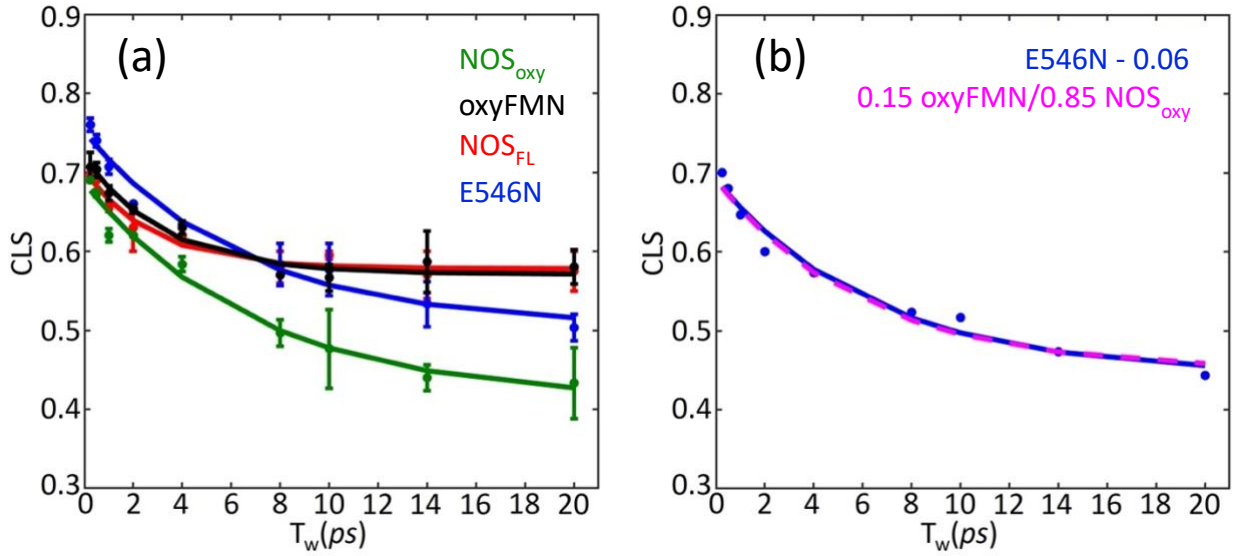

Figure 4. (a) T_w-dependent CLS decay curves (points) and fit (line) of each iNOS protein. Error bars represent standard error from triplicate measurements. (b) Shifted CLS data for $iNOS_{E546N}$ (blue points), fit to exponential function (blue line), and fit to superposition of FFCFs determined for oxyFMN and NOS_{oxy} constructs (dashed magenta line).

Table 1. FFCF parameters from 2D IR spectroscopy and line widths of FT IR spectra for the iNOS constructs.

	Γ (cm^{-1})	**Δ_1 (cm^{-1})**	**τ_1 (ps)**	**Δ_s (cm^{-1})**	**$\Sigma\Delta^2$**	**fwhm[a] (cm^{-1})**
NOS_{oxy}	3.5 ± 0.0	2.1 ± 0.2	10	2.2 ± 0.2	9.3	8.5 ± 0.0
oxyFMN	2.5 ± 0.4	1.4 ± 0.1	3	2.8 ± 0.1	9.8	8.4 ± 0.0
NOS_{FL}	2.5 ± 0.1	1.4 ± 0.1	5	2.8 ± 0.1	9.8	8.4 ± 0.1
NOS_{E546N}	1.9 ± 0.1	1.8 ± 0.1	7	2.5 ± 0.1	9.5	8.3 ± 0.0

[a]full-width-at-half-maximum of linear FT IR spectrum

ASSOCIATED CONTENT

Supporting Information.

The Supporting Information is available free of charge on the ACS Publications website.

Figures S1 – S4, experimental details about protein analysis, spectroscopic measurements and analysis, and UV/visible spectra of NOS constructs (PDF).

AUTHOR INFORMATION

Corresponding Author

*Megan Thielges (thielges@iu.edu)

*Changjian Feng (cfeng@unm.edu)

Author Contributions

The manuscript was written through contributions of all authors. All authors have given approval to the final version of the manuscript.

ACKNOWLEDGEMENT

This material is based upon work funded by NIH GM133973 and NSF 2041692 (CF) and NIH GM114500 and DE-SC0018983 (MCT). This work was also supported in part by National Institutes of Health P20GM130422.

ABBREVIATIONS

NOS, nitric oxide synthase; iNOS, inducible NOS; CaM, calmodulin; NOS_{oxy}, oxygenase domain of NOS; oxyFMN, bi-domain oxygenase/FMN construct in which only the oxygenase and FMN

domains are present, along with the CaM binding region; L-Arg, L-Arginine; H_4B, 6R-5,6,7,8-tetrahydrobiopterin; ET, electron transfer; IET, interdomain electron transfer; wt, wild type; CLS, center line slope; FFCF, frequency-frequency correlation functions; rR, resonance Raman;

References

1. Schmidt, H. H. H. W.; Walter, U., NO at Work. *Cell* **1994**, *78*(6), 919-925.

2. Förstermann, U.; Sessa, W. C., Nitric Oxide Synthases: Regulation and Function. *Eur. Heart. J.* **2012,** 33(7), 829-837.

3. Li, H.; Poulos, T. L., Structure–Function Studies on Nitric Oxide Synthases. *J. Inorg. Biochem.* **2005,** *99* (1), 293-305.

4. Stuehr, D. J.; Haque, M. M., Nitric Oxide Synthase Enzymology in the 20 Years after the Nobel Prize. *British J. Pharmacology* **2019,** *176* (2), 177-188.

5. Cinelli, M. A.; Do, H. T.; Miley, G. P.; Silverman, R. B., Inducible Nitric Oxide Synthase: Regulation, Structure, and Inhibition. John Wiley and Sons Inc.: 2020; Vol. 40, pp 158-189.

6. Sobolewska-Stawiarz, A.; Leferink, N. G. H.; Fisher, K.; Heyes, D. J.; Hay, S.; Rigby, S. E. J.; Scrutton, N. S., Energy Landscapes and Catalysis in Nitric-Oxide Synthase. *J. Biol. Chem.* **2014,** *289* (17), 11725-11738.

7. Li, W.; Fan, W.; Elmore, B. O.; Feng, C., Effect of Solution Viscosity on Intraprotein Electron Transfer Between the FMN and Heme Domains in Inducible Nitric Oxide Synthase. *FEBS Lett.* **2011,** *585* (16), 2622-2626.

8. Hedison, T. M.; Hay, S.; Scrutton, N. S., A Perspective on Conformational Control of Electron Transfer in Nitric Oxide Synthases. *Nitric Oxide* **2017,** *63*, 61-67.

9. Garcin, E. D.; Bruns, C. M.; Lloyd, S. J.; Hosfield, D. J.; Tiso, M.; Gachhui, R.; Stuehr, D. J.; Tainer, J. A.; Getzoff, E. D., Structural Basis for Isozyme-Specific Regulation of Electron Transfer in Nitric-Oxide Synthase. *J. Biol. Chem.* **2004,** *279* (36), 37918-37927.

10. Campbell, M. G.; Smith, B. C.; Potter, C. S.; Carragher, B.; Marletta, M. A., Molecular Architecture of Mammalian Nitric Oxide Synthases. *Proc. Natl. Acad. Sci. U.S.A.* **2014,** *111* (35), E3614-E3614.

11. Feng, C.; Chen, L.; Li, W.; Elmore, B. O.; Fan, W.; Sun, X., Dissecting Regulation Mechanism of the FMN to Heme Interdomain Electron Transfer in Nitric Oxide Synthases. *J. Inorg. Biochem.* **2014**, *130*, 130-140.

12. Feng, C., Mechanism of Nitric Oxide Synthase Regulation: Electron Transfer and Interdomain Interactions. *Coor. Chem. Rev.* **2012,** *256*, 393-411.

13. Smith, B. C.; Underbakke, E. S.; Kulp, D. W.; Schief, W. R.; Marletta, M. A., Nitric Oxide Synthase Domain Interfaces Regulate Electron Transfer and Calmodulin Activation. *Proc. Natl. Acad. Sci. U.S.A.* **2013,** *110* (38), E3577-E3586.

14. Haque, M. M.; Fadlalla, M.; Wang, Z. Q.; Ray, S. S.; Panda, K.; Stuehr, D. J., Neutralizing a Surface Charge on the FMN Subdomain Increases the Activity of Neuronal Nitric-Oxide Synthase by Enhancing the Oxygen Reactivity of the Enzyme Heme-Nitric Oxide Complex. *J. Biol. Chem.* **2009,** *284* (29), 19237-19247.

15. Panda, K.; Haque, M. M.; Garcin-Hosfield, E. D.; Durra, D.; Getzoff, E. D.; Stuehr, D. J., Surface Charge Interactions of the FMN Module Govern Catalysis by Nitric-oxide Synthase. *J. Biol. Chem.* **2006,** *281* (48), 36819-36827.

16. Tejero, J.; Hannibal, L.; Mustovich, A.; Stuehr, D. J., Surface Charges and Regulation of FMN to Heme Electron Transfer in Nitric-Oxide Synthase. *J. Biol. Chem.* **2010,** *285* (35), 27232-27240.

17. Sempombe, J.; Galinato, M. G. I.; Elmore, B. O.; Fan, W.; Guillemette, J. G.; Lehnert, N.; Kirk, M. L.; Feng, C. J. I., Mutation in the Flavin Mononucleotide Domain Modulates Magnetic Circular Dichroism Spectra of the iNOS Ferric Cyano Complex in a Substrate-Specific Manner. *Inorg. Chem.* **2011,** *50* (15), 6859-6861.

18. Hollingsworth, S. A.; Holden, J. K.; Li, H.; Poulos, T. L., Elucidating Nitric Oxide Synthase Domain Interactions by Molecular Dynamics. *Protein Sci.* **2016,** *25*, 374-382.

19. Li, W.; Chen, L.; Lu, C.; Elmore, B. O.; Astashkin, A. V.; Rousseau, D. L.; Yeh, S.-R.; Feng, C., Regulatory Role of Glu546 in Flavin Mononucleotide — Heme Electron Transfer in Human Inducible Nitric Oxide Synthase. *Inorg. Chem.* **2013,** *52* (9), 4795-4801.

20. Astashkin, A. V.; Chen, L.; Elmore, B. O.; Kunwar, D.; Miao, Y.; Li, H.; Poulos, T. L.; Roman, L. J.; Feng, C., Probing the Hydrogen Bonding of the Ferrous-NO Heme Center of nNOS by Pulsed Electron Paramagnetic Resonance. *J. Phys. Chem. A* **2015,** *119* (25), 6641-6649.

21. Jung, C.; Stuehr, D. J.; Ghosh, D. K., FT-Infrared Spectroscopic Studies of the Iron Ligand CO Stretch Mode of iNOS Oxygenase Domain: Effect of Arginine and Tetrahydrobiopterin. *Biochemistry* **2000,** *39* (33), 10163-10171.

22. Phillips, G. N.; Teodoro, M. L.; Li, T.; Smith, B.; Olson, J. S., Bound CO Is a Molecular Probe of Electrostatic Potential in the Distal Pocket of Myoglobin. *J. Phys. Chem. B* **1999,** *103* (42), 8817-8829.

23. Spiro, T. G.; Soldatova, A. V.; Balakrishnan, G., CO , NO and O_2 as vibrational probes of heme protein interactions. *Coord. Chem. Rev.* **2013,** *257* (2), 511-527.

24. Thielges, M. C.; Fayer, M. D., Protein Dynamics Studied with Ultrafast Two-Dimensional Infrared Vibrational Echo Spectroscopy. *Acc. Chem. Res.* **2012,** *45* (11), 1866-1874.

25. Crane, B. R.; Arvai, A. S.; Ghosh, D. K.; Wu, C.; Getzoff, E. D.; Stuehr, D. J.; Tainer, J. A., Structure of Nitric Oxide Synthase Oxygenase Dimer with Pterin and Substrate. *Science* **1998,** *279* (5359), 2121-2121.

26. Sempombe, J.; Elmore, B. O.; Sun, X.; Dupont, A.; Ghosh, D. K.; Guillemette, J. G.; Kirk, M. L.; Feng, C., Mutations in the FMN Domain Modulate MCD Spectra of the Heme Site in the Oxygenase Domain of Inducible Nitric Oxide Synthase. *J. Am. Chem. Soc.* **2009,** *131* (20), 6940-6941.

27. Park, S.; Kwak, K.; Fayer, M. D., Ultrafast 2D-IR Vibrational Echo Spectroscopy: a Probe of Molecular Dynamics. *Laser Phys. Lett.* **2007,** *4* (10), 704-718.

28. Basom, E. J.; Spearman, J. W.; Thielges, M. C., Conformational Landscape and the Selectivity of Cytochrome P450cam. *J. Phys. Chem. B* **2015,** *119* (22), 6620-6627.

29. Ramos, S.; Scott, K. J.; Horness, R. E.; Le Sueur, A. L.; Thielges, M. C., Extended timescale 2D IR Probes of Proteins: *p*-Cyanoselenophenylalanine. *Phys. Chem. Chem. Phys.* **2017,** *19* (15).

30. Kwak, K.; Park, S.; Finkelstein, I. J.; Fayer, M., Frequency-Frequency Correlation Functions and Apodization in Two-Dimensional Infrared Vibrational Echo Spectroscopy: A New Approach. *J. Chem. Phys.* **2007,** *127* (12), 124503-124503.

31. Kwak, K.; Rosenfeld, D. E.; Fayer, M. D., Taking Apart the Two-Dimensional Infrared Vibrational Echo Spectra: More Information and Elimination of Distortions. *J. Chem. Phys.* **2008,** *128* (20), 204505-204505.

32. Hamm, P.; Zanni, M., *Concepts and Methods of 2D Infrared Spectroscopy*. Cambridge University Press: New York, 2011; p 286-286.

33. Fenn, E. E.; Fayer, M. D., Extracting 2D IR Frequency-Frequency Correlation Functions from Two Component Systems. *J. Chem. Phys.* **2011,** *135* (7), 074502-074502.

34. Li, D.; Stuehr, D. J.; Yeh, S.-R.; Rousseau, D. L. Heme distortion modulated by ligand-protein interactions in inducible nitric-oxide synthase. *J. Biol. Chem.* **2004,** *279* (25), 26489-26499.

35. Fan, B.; Wang, J.; Stuehr, D. J.; Rousseau, D. L., NO Synthase Isozymes Have Distinct Substrate Binding Sites. *Biochemistry* **1997,** *36* (42), 12660-12665.

36. Spiro, T. G.; Wasbotten, I., CO as a Vibrational Probe of Heme Protein Active Sites. *J. Inorg. Biochem.* **2005,** *98*, 34-44.

37. Wang, J.; Stuehr, D. J.; Rousseau, D. L., Interactions between Substrate Analogues and Heme Ligands in Nitric Oxide Synthase. *Biochemistry* **1997,** *36* (15), 4595-4606.

38. Das, T. K.; Friedman, J. M.; Kloek, A. P.; Goldberg, D. E.; Rousseau, D. L., Origin of the Anomalous Fe-CO Stretching Mode in the CO complex of Ascaris Hemoglobin. *Biochemistry* **2000,** *39* (4), 837-842.

39. Giroud, C.; Moreau, M.; Mattioli, T. A.; Balland, V.; Boucher, J.-L.; Xu-Li, Y.; Stuehr, D. J.; Santolini, J. J., Role of Arginine Guanidinium Moiety in Nitric-Oxide Synthase Mechanism of Oxygen Activation. *J. Biol. Chem.* **2010,** *285* (10), 7233-7245.

40. Astashkin, A. V.; Chen, L.; Zhou, X.; Li, H.; Poulos, T. L.; Liu, K. J.; Guillemette, J. G.; Feng, C., Pulsed Electron Paramagnetic Resonance Study of Domain Docking in Neuronal Nitric Oxide Synthase: the Calmodulin and Output State Perspective. *J. Phys. Chem. A* **2014,** *118* (34), 6864-6872.

41. Ghosh, D. K.; Ray, K.; Rogers, A. J.; Nahm, N. J.; Salerno, J. C., FMN Fluorescence in Inducible NOS Constructs Reveals a Series Of Conformational States Involved in the Reductase Catalytic Cycle. *FEBS J.* **2012,** *279* (7), 1306-1317.

42. Sheng, Y.; Zhong, L.; Guo, D.; Lau, G.; Feng, C., Insight into Structural Rearrangements and Interdomain Interactions Related to Electron Transfer Between Flavin Mononucleotide and Heme

in Nitric Oxide Synthase: A Molecular Dynamics Study. *J. Inorg. Biochem.* **2015,** *153* (239), 186-196.

43. Merchant, K. A.; Noid, W. G.; Akiyama, R.; Finkelstein, I. J.; Goun, A.; McClain, B. L.; Loring, R. F.; Fayer, M. D., Myoglobin-CO Substate Structures and Dynamics: Multidimensional Vibrational Echoes and Molecular Dynamics Simulations. *J. Am. Chem. Soc.* **2003,** *125* (45), 13804-18.

44. Massari, A. M.; Finkelstein, I. J.; McClain, B. L.; Goj, A.; Wen, X.; Bren, K.; Loring, R. F.; Fayer, M. D., The Influence of Aqueous versus Glassy Solvents on Protein Dynamics: Vibrational Echo Experiments and Molecular Dynamics Simulations. *J. Am. Chem. Soc.* **2005,** *127*, 14279-14289.

45. Finkelstein, I. J.; Massari, A. M.; Fayer, M. D., Viscosity-Dependent Protein Dynamics. *Biophys. J.* **2007,** *92* (10), 3652-3662.

46. King, J. T.; Arthur, E. J.; Brooks, C. L.; Kubarych, K. J., Site-Specific Hydration Dynamics of Globular Proteins and the Role of Constrained Water in Solvent Exchange with Amphiphilic Cosolvents. *J. Phys. Chem. B* **2012,** *116* (19), 5604-5611.

47. King, J. T.; Arthur, E. J.; Brooks 3rd, C. L.; Kubarych, K. J., Crowding Induced Collective Hydration of Biological Macromolecules over Extended Distances. *J. Am. Chem. Soc.* **2014,** *136* (1), 188-194.

48. Page, C. C.; Moser, C. C.; Dutton, P. L., Mechanism For Electron Transfer within and between Proteins. *Curr. Opin. Chem. Biol.* **2003,** *7* (5), 551-556.

49. Lin, J.; Balabin, I. A.; Beratan, D. N., Chemistry: The nature of Aqueous Tunneling Pathways between Electron-Transfer Proteins. *Science* **2005,** *310* (5752), 1311-1313.

50. Gray, H. B.; Winkler, J. R., Electron Flow through Metalloproteins. *Biochim. Biophys. Acta* **2010,** *1797* (9), 1563-72..

51. Skourtis, S. S.; Waldeck, D. H.; Beratan, D. N., Fluctuations in Biological and Bioinspired Electron-Transfer Reactions. *Annu. Rev. Phys. Chem.* **2010,** *61*, 461-485.

52. LeBard, D. N.; Matyushov, D. V., Glassy Protein Dynamics and Gigantic Solvent Reorganization Energy of Plastocyanin. *J. Phys. Chem. B* **2008,** *112* (16), 5218-5227.

53. LeBard, D. N.; Matyushov, D. V., Ferroelectric Hydration Shells around Proteins: Electrostatics of the Protein-Water Interface. *J. Phys. Chem. B* **2010,** *114* (28), 9246-9258.

54. Krishtalik, L. I., The Medium Reorganization Energy for the Charge Transfer Reactions in Proteins. *Biochim. Biophys. Acta Bioenerg.* **2011,** *1807* (11), 1444-1456.

TOC Graphic